© 2019. Published by The Company of Biologists Ltd.

Mitochondrial NCKX5 regulates melanosomal biogenesis and pigment production

Zhao Zhang[1, 2, 3], Juanjuan Gong[2], Elena V. Sviderskaya[4], Aihua Wei[5 *], Wei Li[2, 6 *]

[1] State Key Laboratory of Molecular Developmental Biology, Institute of Genetics and Developmental Biology, Chinese Academy of Sciences, Beijing 100101, China

[2] Beijing Key Laboratory for Genetics of Birth Defects, Beijing Pediatric Research Institute; MOE Key Laboratory of Major Diseases in Children; Genetics and Birth Defects Control Center, National Center for Children's Health; Beijing Children's Hospital, Capital Medical University, Beijing 100045, China

[3] University of Chinese Academy of Sciences; Beijing 100039, China

[4] Cell Signalling Research Centre, St. George's, University of London, London, SW17 0RE, UK

[5] Department of Dermatology, Beijing Tongren Hospital, Capital Medical University, Beijing 100730, China

[6] Shunyi Women and Children's Hospital of Beijing Children's Hospital, Beijing 101300, China.

* Correspondence to **Dr. Wei Li**, Beijing Children's Hospital, Capital Medical University, Beijing 100045. Tel: +86-10-5961-6628, Fax: +86-10-5971-8699, Email: liwei@bch.com.cn; **Dr. Aihua Wei**, Department of Dermatology, Beijing Tongren Hospital, Capital Medical University, Beijing 100730, China. Tel/Fax: +86-10-5826-8092, Email: weiaihua3000@163.com.

Journal of Cell Science • Accepted manuscript

JCS Advance Online Article. Posted on 14 June 2019

Summary statement

Mitochondrial NCKX5 plays a key role in regulating melanogenesis through organelle interaction, which is implicated in graying hair in aged people or hypopigmented lesions in vitiligo patients.

Abstract

Oculocutaneous albinism (OCA) is a heterogeneous and autosomal recessive hypopigmentation disorder, which is caused by mutations of genes involved in pigment biosynthesis or melanosome biogenesis. We have identified *NCKX5* or *SLC24A5* as a causative gene for OCA6. However, the pathogenesis of OCA6 is unknown. We found that NCKX5 is localized to mitochondria, not to melanosomes. Pharmacological inhibition of mitochondrial function or NCKX exchanger activity reduced pigment production. Loss of NCKX5 attenuated Ca^{2+} enrichment in melanosomes which compromised PMEL fibril formation, melanosome maturation and pigment production. Thus, we have defined a new class of hypopigmentation attributable to dysfunctional mitochondria by impairing mitochondrial Ca^{2+} transfer into melanosomes, which is implicated in graying hair in aged people or hypopigmented lesions in vitiligo patients.

KEY WORDS: melanosome; mitochondrion; NCKX5/SLC24A5; oculocutaneous albinism; pigment

Journal of Cell Science • Accepted manuscript

INTRODUCTION

Albinism is a rare inherited disease characterized by poor vision and variable hypopigmentation manifestations. The absence or reduction in pigment occurs in the skin, hair, and eyes (oculocutaneous albinism, OCA) or mainly in the eyes (ocular albinism, OA) (Li et al., 2006). At least 18 genes have been identified as causative genes for human albinism. These include six nonsyndromic OCA genes, *TYR* (OCA1), *OCA2* (OCA2), *TYRP1* (OCA3), *SLC45A2* (OCA4), *SLC24A5* (OCA6), *C10ORF11* (OCA7), and one single gene associated with OA, *GPR143* (OA1). Moreover, there are additional eleven syndromic OCA genes, including ten Hermansky–Pudlak syndrome (HPS) genes, *HPS1*(HPS1), *AP3B1* (HPS2), *HPS3* (HPS3), *HPS4* (HPS4), *HPS5*(HPS5), *HPS6* (HPS6), *DTNBP1* (HPS7), *BLOC1S3* (HPS8), *BLOC1S6* (HPS9), *AP3D1* (HPS10), and one Chediak–Higashi syndrome (CHS) gene, *LYST* or *CHS1* (Ammann et al., 2016; Li et al., 2006; Wei and Li, 2013).

Currently, OCA is categorized into two groups. One is the lack of melanosomal proteins, such as tyrosinase, OCA2, or TYRP1 which leads to non-syndromic OCA1~3 subtypes, respectively. The other is the deficiency of melanosomal transporting complexes, such as HPACs (HPS Protein Associated Complexes), which leads to defective melanosomes in HPS. Syndromic OCA is often accompanied by disrupted biogenesis of a group of lysosome-related organelles (LROs), including melanosomes in melanocytes, dense granules in platelets, lamellar bodies in lung type 2 epithelial cells, exhibiting additional symptoms such as prolonged bleeding, and fatal lung disease in some cases (Wei and Li, 2013). We adopted whole-exome sequencing with a family-based recessive mutation model and determined that

Journal of Cell Science • Accepted manuscript

SLC24A5 was a newly defined causative gene for nonsyndromic OCA which has been designated as OCA6 (Wei et al., 2013). The human *SLC24A5* gene, encodes a member of the K^+-dependent Na^+/Ca^{2+} exchanger family, NCKX5 (Lamason et al., 2005). Endogenous human NCKX5 is partially localized to the trans-Golgi network (TGN) (Ginger et al., 2008). Proteomics analysis reveals that NCKX5 is present in melanosomes (Chi et al., 2006), suggesting it is a melanosomal protein (Ito and Wakamatsu, 2011). However, the precise melanosomal localization of NCKX5 in melanocytes is lacking. It is unclear whether NCKX5 is a melanosomal protein or is associated with any melanosomal transporting complexes. Thus, which group of OCA that OCA6 falls in remains unsettled.

Melanosomes can be morphologically classified into four distinct stages (I-IV) based on the degree of maturation (Sitaram and Marks, 2012). Melanosomes originate from recycling endosomes (Raposo et al., 2001). Melanosomal scaffolding protein PMEL is a driving force for premelanosome fibril formation (Berson et al., 2001; Kushimoto et al., 2001; Raposo et al., 2001). Processing of PMEL is mediated by a furin-like protease, whose activity is highly calcium-dependent (Thomas, 2002). However, the origin of melanosomal Ca^{2+} is unknown. Several organelles such as the ER, mitochondria and lysosomes are highly enriched with Ca^{2+}. The ER is believed to be the major intracellular Ca^{2+} pool for supplying Ca^{2+} to other organelles (Burgoyne et al., 2015). Domains between the ER and mitochondria called MAMs (mitochondria-associated membranes) (Vance, 1990), selectively transfer Ca^{2+} from the ER to mitochondria (Rizzuto et al., 2009; Rizzuto et al., 1998). Melanosomes are acidic organelles containing high Ca^{2+} levels (Bush and Simon, 2007; Hoogdijn et al., 2003; Patel and Docampo, 2010). The melanosome is a member of LROs (Wei and Li, 2013). Likewise,

Journal of Cell Science • Accepted manuscript

lysosomes and other acidic LROs similarly store Ca^{2+} (Patel and Docampo, 2010). It was recently reported that lysosomal Ca^{2+} originates from the ER (Garrity et al., 2016). However, the source of Ca^{2+} for LROs remains uncertain. LRO Ca^{2+} is thought to originate either from organelle contacts with the ER or from cytosol by Ca^{2+} transporters, driven by ATP hydrolysis (Patel and Docampo, 2010). In fact, cytosolic Ca^{2+} is relatively low in resting condition (Berridge et al., 2000). Ca^{2+} in the ER or other Ca^{2+} enriched organelles could be transferred to LROs by physical contacts with these organelles. The connections between mitochondria and melanosomes are morphologically similar to the ER-mitochondria contacts, and are also modulated by a fusion player MFN2 (Daniele et al., 2014). We therefore hypothesize that melanosome-mitochondria contact sites may serve as exchanging sites for Ca^{2+}.

There exist two families of Na^{+}/Ca^{2+}exchangers, the K^{+}-independent Na^{+}/Ca^{2+} exchanger family (NCX) and the K^{+}-dependent Na^{+}/Ca^{2+} exchanger family (NCKX) (Blaustein and Lederer, 1999). NCKX5 possesses NCKX activity in a heterologous expression system (Ginger et al., 2008). In this study, we found that NCKX5 enriched in mitochondria and we further defined that mitochondrial NCKX5 plays an important role in regulating melanosomal Ca^{2+} homeostasis that is required for melanosome maturation and pigment production, which explains the pathogenesis of OCA6.

RESULTS

NCKX5 is localized to mitochondria and TGN, but not to melanosomes

As the precise subcellular localization of NCKX5 is controversial, we sought to determine the exact subcellular localization of NCKX5 in melanocytes. A full-length mouse *Nckx5* transgene with a myc-epitope tag inserted in-frame into the protein

Journal of Cell Science • Accepted manuscript

(NCKX5-myc) was generated. When expressed in melan-a melanocytes, NCKX5-myc did not colocalize with PMEL (an immature melanosomal marker) (**Fig. 1a-a"**) or TYRP1 (a mature melanosomal marker) (**Fig. 1b-b"**). In addition, NCKX5-myc did not colocalize with pigment granules visualized by bright-field microscopy (**Fig. 1c-c"**). However, we observed partial co-labeling of NCKX5-myc with a trans-Golgi network (TGN) marker TGN38 (**Fig. 1d-d"**), confirming that NCKX5 is partially localized to the TGN (Ginger et al., 2008). To our surprise, transient transfected NCKX5-myc largely colocalized with a mitochondrial marker cytochrome c (**Fig. 1e-e"**). To confirm this result, we detected endogenous NCKX5 localization by labeling the melan-a melanocytes with three different NCKX5 polyclonal antisera (**Fig. 1f**). Consistent with the overexpressed NCKX5-myc, the endogenous NCKX5 colocalized with mitochondrial protein cytochrome c as well (**Fig. 1g-i"**). Almost in all observed melan-a melanocytes, the endogenous NCKX5 detected by NCKX5-C4 polyclonal antisera exhibited a mitochondrial distribution pattern (**Fig. 1j-k"**). Whereas in some melanocytes (~30%) the overexpressed NCKX5-myc did not localize to mitochondria by only localizing at the perinuclear area with a TGN distributional pattern (**Fig. 1l-n**). Nevertheless, our immunofluorescence microscopy (IFM) results suggest that NCKX5 is localized to mitochondria and TGN, but not to melanosomes in melan-a melanocytes.

Journal of Cell Science • Accepted manuscript

Disruption of NCKX5 compromises melanosomal Ca^{2+} concentration, melanosomal PMEL expression and melanin production

We next investigated how NCKX5 functions in pigment production in melanocytes. Western blot analysis showed that melan-a melanocytes treated with NCKX5-specific siRNA (NCKX5-KD) dramatically decreased the expression of NCKX5 (**Fig. 2a**). Consequently, melanin production was greatly reduced in NCKX5-KD (knockdown) melanocytes, which was restored by expressing exogenous NCKX5-myc (**Fig. 2b-g**), but not by the reported mutant L454Ffs31X-myc and S182R-myc (Morice-Picard et al., 2014; Wei et al., 2013) (data not shown), confirming the reduced pigmentation in the OCA6 patient with loss of NCKX5 (Wei et al., 2013).

NCKX5 has the Na^{+}/Ca^{2+} exchanger activity in a heterologous expression system (Ginger et al., 2008). We therefore reasoned that NCKX5 may affect melanosomal Ca^{2+} homeostasis in some way. To detect melanosomal Ca^{2+}, we engineered the genetically modified Ca^{2+} sensor GCaMP6 to the N-terminus of tyrosinase, which is expressed on the luminal side of the melanosome membrane. Indeed, NCKX5- KD cells exhibited a reduced level of GCaMP6 fluorescence intensity, indicative of lower lumenal Ca^{2+} concentration compared with wild-type (WT) cells (**Fig. 2h-l**).

Melanosomal scaffolding protein PMEL is cleaved by a furin-like protease to form PMEL fibrils, which is strictly Ca^{2+} dependent (Berson et al., 2003; Thomas, 2002). We speculate that reduced melanosome Ca^{2+} level may disrupt PMEL processing. A monoclonal antibody HMB45, which specifically recognizes the luminal fragment of PMEL (Hoashi et al., 2006; Yasumoto et al., 2004), is used for monitoring fibrillar

Journal of Cell Science • Accepted manuscript

formation of PMEL, a critical step in melanosome biogenesis. IFM analysis showed that PMEL puncta were observed in control (ctrl) cells, but were invisible in NCKX5- KD cells (**Fig. 2m-n**). In addition, fibril-enriched detergent-insoluble PMEL was not detectable in NCKX5- KD cells by immunoblotting assay (**Fig. 2r**). These results are consistent with that disruption of PMEL sorting and processing leads to the degradation of PMEL luminal domain together with the transmembrane fragment (Niel et al., 2011), confirming the reduction of matured melanosomes in the skin melanocytes of the OCA6 patient (Wei et al., 2013).

There exist two families of Na^+/Ca^{2+}exchangers, NCX and NCKX family (Blaustein and Lederer, 1999). The NCKX family consists of five members. While the NCKX1~4 proteins are mainly localized to the plasma membrane (Schnetkamp, 2013), NCKX5 is localized to mitochondria and TGN in melanocytes (as shown in **Fig. 1**). However, it has been reported that Ca^{2+} efflux from mitochondria is mediated by another Na^+/Ca^{2+} exchanger, NCLX, a member of the NCX family (Luongo et al., 2017; Palty et al., 2010). We therefore tested whether NCLX or NCKX activity is required for melanogenesis. We treated cells with a NCKX inhibitor DBZ (Altimimi et al., 2013; Shumilina et al., 2010) and a NCX inhibitor CGP-37157 (Cox et al., 1993; Palty et al., 2010), respectively. IFM analysis showed that the number of PMEL puncta was decreased by DBZ, but less affected by CGP-37157 (**Fig. 2o-q**). Immunoblotting assays showed that the intensity of low molecular band of PMEL was specifically decreased, and the high molecular band of PMEL was apparently increased by DBZ treatment but not by CGP-37157 treatment (**Fig. 2r**), suggesting that disruption of NCKX but not NCX

Journal of Cell Science • Accepted manuscript

activity compromises proteolytic processing of PMEL, thereby leads to an accumulation of its precursor. Together, these results suggest that NCKX5 possesses the NCKX activity and plays a key role in regulating melanosomal Ca^{2+} homeostasis and thus regulates PMEL processing, melanosome maturation and pigment production.

Ca^{2+} indicators, rhod-2 and X-rhod-1, efflux from mitochondria and influx into melanosomes in a time-dependent manner

Previous findings have shown physical contacts between mitochondria and melanosomes (Daniele et al., 2014). These contacts are morphologically similar to ER-mitochondria tethers, which may selectively transfer Ca^{2+} from ER to mitochondria (Giorgi et al., 2009; Patergnani et al., 2011). As NCKX5 is enriched in mitochondria and regulates melanosomal Ca^{2+} level (**Fig. 1 and 2h-l**), we speculated that mitochondrial Ca^{2+} might be transferred to melanosomes in a similar manner. It is hard to trace the flow of free Ca^{2+} ion between organelles. We monitored this exchange in an indirect method. Rhodamine-2/acetoxymethyl ester (rhod-2/am) is a widely used Ca^{2+}-tracer. Esterolysis of the permeant cation rhod-2/am generates zwitterionic rhod-2, which is trapped in mitochondria (Minta et al., 1989), to represent mitochondrial Ca^{2+} (Fonteriz et al., 2010; Kostic et al., 2015; Palty et al., 2010). Cells transfected with mito-GFP were incubated with rhod-2/am for 30 minutes for dye loading and then were washed with excessive fresh medium. After incubation with a standard medium for 20 minutes, we observed that the filamentous rhod-2 signals were mainly colocalized with mito-GFP in melan-a melanocytes analyzed by IFM (**Fig. 3a-a"**). At 40 minutes, a proportion of the rhod-2

Journal of Cell Science • Accepted manuscript

signals became punctate that were not co-labeled with mito-GFP (**Fig. 3b-b”**). At 60 minutes, rhod-2 signals were almost completely punctate and separated from mito-GFP positive mitochondria (**Fig. 3c-c”**). The colocalization between mito-GFP and rhod-2 fluorescence was dramatically decreased during the observation period (**Fig. 3d**). Furthermore, time course images also showed that the mitochondria-localized rhod-2 signals gradually faded, and the dot-like rhod-2 signals separated from mito-GFP labeled mitochondria at the same time (**Fig. 3i**). These results suggest that Ca^{2+}-bound rhod-2 is gradually effluxed from mitochondria.

We next transfected the melanocytes with MART1-GFP, a protein enriched in immature melanosome (Hoashi et al., 2005), to trace the flux of rhod-2 fluorescence. The colocalization of MART1-GFP and rhod-2 fluorescence was apparently increased during the observation period (**Fig. 3e-h**). Furthermore, time course images also showed that the dot-like rhod-2 signals gradually colocalized with MART1-GFP labeled melanosomes (**Fig. 3j**), suggesting that rhod-2 fluorescence is influxed into melanosomes in a time-dependent manner. In addition, the rhod-2 positive dots visualized by bright field (BF) microscopy overlapped well with pigment granules (**Fig. 3k-m**), confirming that the punctate dots are melanosomes.

If the rhod-2 signal is transferred from mitochondria to melanosomes, disruption of rhod-2/am loading into mitochondria would compromise subsequent rhod-2 fluorescence accumulation in melanosomes. The rhod-2/am within mitochondria is membrane potential dependent (Babcock et al., 1997). We treated the cells with carbonyl cyanide m-chlorophenyl hydrazone (CCCP) to dissipating mitochondrial transmembrane potential

Journal of Cell Science • Accepted manuscript

(Ding et al., 2010). Indeed, compared to control cells, CCCP-treated cells completely lost mitochondrial specific rhod-2 signals as well as the melanosomal punctate rhod-2 signals (**Fig. 4a-b, d-e, g-h, j**). After washout of CCCP, the mitochondrial rhod-2 signals restored to some extent (**Fig. 4c**). Subsequently, the melanosomal rhod-2 signals largely re-appeared (**Fig. 4f, i, j**). In addition, we tested whether disruption of mitochondrial normal physiological functions would impede rhod-2 dynamics. We inhibited mitochondrial oxidative phosphorylation by treating melanocytes with oligomycin and rotenone, respectively. In oligomycin-treated cells, the majority of rhod-2 signals constantly co-localized with mito-GFP, and much fewer punctate rhod-2 dots were separated from mito-GFP (**Fig. 4k, l, j**), suggesting that rhod-2 is retained in mitochondria, precluding its transfer to melanosomes. In oligomycin washout cells, the rhod-2 signals were punctate and were clearly separated from mito-GFP resembling the control group (**Fig. 4j, m**). Rotenone has similar inhibitory effects in melanocytes (**Fig. 4j**). Taken together, these results suggest that rhod-2 is transferred from mitochondria into melanosomes in melan-a melanocytes, which is dependent on functional mitochondria.

Similar to rhod-2, another Ca^{2+} tracer X-rhod-1 could be transferred from mitochondria to melansomes (**Fig. 5 a, c, e, g, j, k**). In contrast, mitochondrial dyes mitotracker CMXRos and an analog of rhod-2/am, rhodamine 123, which possess similar fluorophores to X-rhod-1 or rhod-2 but lack of Ca^{2+} binding radical, were constantly trapped in mitochondria (**Fig. 5 b, d, f, h**). These results suggest that the Ca^{2+} binding fluorophores are required for the specific transfer of X-rhod-1 or rhod-2 from mitochondria to melanosomes. This establishes a unique tool for monitoring the transfer

Journal of Cell Science • Accepted manuscript

of mitochondrial Ca^{2+} signal into melanosomes or other Ca^{2+} enriched organelles (data not shown). Our results suggest that ions such as Ca^{2+} are likely influxed into melanosomes from mitochondria which provide another source of Ca^{2+}.

Disruption of NCKX5 and NCKX activity compromise rhod-2 loading in melanosomes and pigment production

To test whether loss of NCKX5 affects Ca^{2+} flow from mitochondria to melanosomes in melanocytes, NCKX5-KD cells were transfected with mito-GFP or MART1-GFP to trace the subcellular localization of rhod-2 fluorescence. In control cells, the rhod-2 fluorescence overlapped with mito-GFP at the beginning and then with MART1-GFP during the observation period (**Fig. 6a, e**). In contrast, in NCKX5-KD cells, rhod-2 fluorescence overlapped with mito-GFP at the beginning, while much fewer rhod-2 puncta overlapped with MART1-GFP during the observation period and the intensity was decreased (**Fig. 6b, f, i**), suggesting that Ca^{2+} signal flow from mitochondria to melanosomes is impeded. These results are consistent with the reduced melanosomal Ca^{2+} concentration measured by GCaMP6-TYR in NCKX5-KD cells (**Fig. 2h-l**).

Consistent with our findings of impaired PMEL processing in NCKX5-KD cells (shown in **Fig. 2o-r**), NCKX inhibitor DBZ did not disrupt rhod-2 releasing from mitochondria, but attenuated rhod-2 accumulation in melanosomes (**Fig. 6c, g, j**), suggesting that the NCKX activity is required for Ca^{2+} transfer from mitochondria to melanosomes. On the contrary, NCLX inhibitor CGP-37157 retained rhod-2 signals in mitochondria, but did not attenuate rhod-2 accumulation in melanosomes (**Fig. 6d, h, k**),

Journal of Cell Science • Accepted manuscript

consistent with the finding that blocking NCLX activity likely inhibits mitochondrial Ca^{2+} extrusion into cytosol (Palty et al., 2010). Furthermore, NCKX activity depends on the K^+ gradient in exchange of Ca^{2+} (Schnetkamp, 2013). We speculate that depletion of K^+ in the medium may attenuate the efflux of rhod-2 signals. Indeed, K^+ deprivation did not influence the rhod-2 signal separation from mito-GFP labeled mitochondria, but apparently attenuated rhod-2 accumulation in melanosomes. The number of rhod-2-loaded melanosomes was dramatically reduced along with sequential declining K^+ levels (**Fig. 7**), suggesting that K^+ deprivation does not block the Ca^{2+} efflux from mitochondria, but may attenuate Ca^{2+} signal accumulation in melanosomes. Taken together, our results suggest that NCKX5 and NCKX activity are required for Ca^{2+} signal flow from mitochondria to melanosomes.

Consistent with the inhibitory effects on mitochondrial Ca^{2+} transfer to melanosomes, we observed a dramatic inhibition of melanin synthesis in the DBZ-treated but not in the CGP-37157-treated melanocytes (**Fig. 8a-d, i**), suggesting that NCKX but not NCX activity is required for melanogenesis. In addition, CCCP, oligomycin, or rotenone treated cells exhibited an apparent reduction of melanin content. In contrast, the lysosomal protease inhibitor leupeptin (Niel et al., 2011) had no obvious inhibitory effect on melanin synthesis (**Fig. 8e-h, j**). These results suggest that functional mitochondria and the NCKX activity are required for melanogenesis, which establishes the functional link between mitochondria and melanosomes.

Journal of Cell Science • Accepted manuscript

Taken together, our data suggest that there exist substance exchanges between mitochondria and melanosomes, and loss of mitochondrial NCKX5 likely attenuated Ca^{2+} enrichment in melanosomes which compromised melanosome maturation and pigment production.

DISCUSSION

Previous studies demonstrated that NCKX5 may be localized to TGN or melanosomes, we here have shown that NCKX5 is localized to mitochondria and TGN (but not melanosomes) in melanocytes. Several studies have reported the subcellular localization of NCKX5 in pigment cells, but conflicting data has been presented. In human melanoma MNT1 cells, GFP-tagged and HA-tagged zebrafish NCKX5 exhibited an intracellular localization (Lamason et al., 2005). There was no organellar marker co-labelled in the MNT1 cells, but the distributional pattern did not look like a TGN pattern. Proteomic analysis in MNT1 cells reveals that NCKX5 is present in melanosomes (Chi et al., 2006). However, they also estimated that melanosome fractions are contaminated with 1-6% mitochondrial proteins. Similarly, we also found that the mitochondrial fraction in melanocytes was always dark, which is indicative of mixture of melanosomes (data not shown). This suggests that mitochondria and melanosomes may have overlapping sediment features and co-exist largely in the same fraction, which may explain the identification of NCKX5 in melanosomes by proteomic analysis (Chi et al., 2006). Unfortunately, they did not prove its melanosomal localization by IFM. In normal human epidermal melanocytes (NHM), endogenous human NCKX5, which was detected by polyclonal antisera, was reported to be partially localized to

Journal of Cell Science • Accepted manuscript

TGN (Ginger et al., 2008). The authors did not mention the additional signals outside of TGN. Our investigation indicated the additional signals were localized to mitochondria. Recently, overexpressed NCKX5 has been reported to be exclusively located in TGN in MNT1 cells (Rogasevskaia et al., 2019). We have shown an exclusive TGN localization of overexpressed NCKX5 in about 30% melanocytes (**Fig. 1l-n**). Therefore, we concluded that NCKX5 localizes to both TGN and mitochondria, but not to melanosomes. Considering that TGN-localized NCKX5 is transported by the secretory pathway, whereas the mitochondrial NCKX5 is not, we speculate that there may exist two isoforms of NCKX5, with or without the predicted N-terminal 29-residue signal peptide. However, this awaits further investigation.

In this study, we have demonstrated that mitochondrial NCKX5 plays a pivotal role in regulating melanogenesis, although we have not excluded a possible contribution of the TGN-localized NCKX5 to melanogenesis. The pathogenesis of OCA has been classified into two categories. One lacks melanosomal protein; the other is deficient in melanosomal protein trafficking complexes (Wei and Li, 2013). We have excluded the melanosomal localization of NCKX5. The transmembrane features of NCKX5 argue that it behaves like a trafficking protein for melanosomal proteins. Thus, we have defined a new class of OCA caused by dysfunctional mitochondria, which we refer it as “mitochondrial OCA”. With this regard, it is predicted that deficiency in other mitochondrial components coupling with NCKX5 or for mitochondrial homeostasis could likewise produce a hypopigmentation phenotype. We confirmed that NCKX5 is partially localized to TGN, but the physiological functions of TGN-targeted NCKX5 need further investigation.

Journal of Cell Science • Accepted manuscript

There are several hypotheses on the graying of hair with aging, ranging from melanocyte and melanogenic stem cell death to reduction in melanin synthesis. Reactive oxygen species (ROS)-induced damage has been suggested. However, the precise mechanism(s) remain unknown (Seiberg, 2013). Mitochondria, are both a major source and a primary target of toxic ROS within cells, especially when excessive ROS is produced during melanogenesis, thus playing a pivotal role in aging and stress sensing (Harman, 1972). Similarly, in some vitiligo patients, melanocytes and melanosomes exist but pigment production is inhibited (Ezzedine et al., 2015). Mitochondrial function is impaired in vitiligo melanocytes (Dell'Anna et al., 2001; Laddha et al., 2013). Inhibition of mitochondrial function may explain the hypopigmentation in these aged and/or stressed melanocytes.

Mitochondrion-melanosome contact sites may have functions in exchanging Ca^{2+} and other molecules such as ATP, lipids or proteins required for melanosome biogenesis or melanin biosynthesis. NCKX5 may acts as a key mitochondrial Ca^{2+} effluxer and is important for Ca^{2+} homeostasis within both mitochondria and melanosomes. It is unknown whether NCKX5 localizes at the mitochondrion-melanosome contact sites, coupled with another Ca^{2+} influxer on melanosomes, to directly mediate Ca^{2+} transport. This machinery awaits further investigation. Our findings expand our knowledge of the functions of the mitochondrial interactome, indicating that mitochondrion is another organellar Ca^{2+} source through the organelle interactions.

Journal of Cell Science • Accepted manuscript

MATERIALS AND METHODS

DNA constructs

The full-length cDNA of mouse *Nckx5* was amplified from melan-a total RNA. To construct pNCKX5, the entire *Nckx5* cDNA was subcloned into the *EcoR*I and *Xho*I sites of pcDNA3.1(+) (Invitrogen). To generate epitope-tagged pNCKX5, the myc-epitope tag was inserted between Ser-52 and Glu-53 of the NCKX5 to generate pNCKX5-myc based on a scheme of a previous study (Ginger et al., 2008). The full-length cDNA of mouse *Mart1* was amplified from melan-a total RNA. To construct MART1-GFP, the entire *Mart1* cDNA was subcloned into the *Xho*I and *EcoR*I sites of pEGFP-N2 (Clontech). The cDNA of mouse *Cox8a* was amplified from mouse liver total RNA. To construct mito-GFP, the signal peptide of Cox8a, corresponding to amino acids 1-25, was subcloned into the *Xho*I and *EcoR*I sites of pEGFP-N2 (Clontech). The full-length cDNA of mouse *tyrosinase* was amplified from melan-a total RNA. To construct GCaMP6-TYR, the entire *tyrosinase* cDNA was subcloned into the *Hind*III and *Xbal*I sites of pGP-CMV-GCaMP6m (Addgene).

Generation of NCKX5 knockdown (KD) melan-a melanocytes

Small hairpin RNAs (shRNA) against mouse *Nckx5* gene (NCBI RefSeq NM_175034.3) were designed by the siRNA target finder (Ambion, Austin, TX). Oligodeoxyribonucleotide duplexes containing the target sequences were synthesized and introduced into the *BamH* I and *Hind* III sites of the expression plasmid pSilencer 5.1-H1

Journal of Cell Science • Accepted manuscript

Retro vector (Ambion). The target sequences were as follows: shNCKX5, 5′-GCTGGAAACTAGACCGAAA-3′, and for scramble control, 5'-AATTCTCCGAACGTGTCACGT-3'. To generate shRNA-resistant NCKX5, 5 silent mutations were introduced into pNCKX5-myc by site-directed mutagenesis, changing the sites from GGCTGGAAACTAGACCGAAAG to GGCTGGAAGTTGGATAGAAAG (silent mutations are underlined). Melan-a melanocytes were seeded in a 35×10 mm dish at 2.0×10^5 cells 24 hours prior to transfection. The vectors were transfected into cells using Fugene 6 (Promega) following the manufacturer's instructions. After 24 hours, the transfected cell clone expressing the vector was selected by 2.5 mg/ml of puromycin (Invivogen).

Cell culture and transfections

Immortalized melan-a melanocytes (Bennett et al., 1987) were obtained from the Wellcome Trust Functional Genomics Cell Bank. Melan-a cells were grown at 37°C and 10% CO_2 in RPMI 1640 (Hyclone), 10% fetal bovine serum (FBS) (Hyclone), 1% penicillin/streptomycin (P/S), 200 nM phorbol 12-myristate-13-acetate (Sigma). NCKX5-KD melanocytes were maintained in RPMI 1640, 10% FBS, 1% P/S, 200 nM phorbol 12-myristate-13-acetate and 2 mg/ml puromycin (InvivoGen). Melan-a melanocytes were transfected by using Fugene 6 (Promega) according to manufacturer's instructions with 1~2 μg of DNA. NCKX5-KD cells were transfected by using Neon transfection system (Life Technologies) according to manufacturer's instructions with 1~2 μg of DNA.

Journal of Cell Science • Accepted manuscript

Antibodies

NCKX5-A1 polyclonal anti-sera were generated in rabbits against synthetic peptides corresponding to amino acids 253-268 of the mouse NCKX5. NCKX5-B1 polyclonal anti-sera were generated in rabbits against synthetic peptides corresponding to amino acids 492-501 of the mouse NCKX5. NCKX5-C4 polyclonal anti-sera against mouse NCKX5 was generated by immunizing rabbits with a purified His-tagged fusion protein corresponding to amino acids 210-306 of the mouse NCKX5. The following antibodies were used in this study: mouse anti-TYRP1 (Covance, MEL5, 1:500), mouse anti-cytochrome c (BD, 556432, 1:1,000), mouse anti-PMEL (Thermo, HMB45,1:200), mouse anti-Myc (Huaxingbio, HX1802, 1:1000), rabbit anti-Myc (MBL, 562, 1:500), rat anti-LAMP1 (BD, 553792, 1:500), rabbit anti-TGN38 (Santa Cruz, sc-33784, 1:200), mouse anti-β-actin (Sigma, A5441, 1:20,000).

Immunoblotting

Immortalized melanocytes were washed with ice-cold PBS, re-suspended in lysis buffer (50 mM Tris-HCl pH 7.4, 150 mM NaCl, 1% Triton X-100) in the presence of a protease inhibitor cocktail (Sigma-Aldrich). After 60 minutes incubation on ice, cell lysates were centrifuged at 13,000 g for 15 minutes at 4°C to remove cell debris. Equal amounts of homogenates were separated on 10% SDS-PAGE gels and transferred onto polyvinylidene difluoride (PVDF, Millipore) membranes. The membrane was then blocked with blocking buffer (5% skimmed milk and 0.1% Tween 20 in PBS) and incubated with primary antibody overnight at 4°C. Blots were incubated with the

Journal of Cell Science • Accepted manuscript

appropriate HRP-conjugated secondary antibodies for 1.5 h at room temperature, and visualized by ECL (Pierce, Rockford, IL).

Immunofluorescence microscopy

Mouse melanocytes were seeded at 0.5×10^5 per well in 12-well dishes on coverslips. After overnight, cells were transfected with expressing plasmids for 24~48 hours. After washing twice with PBS, cells were fixed with 4% (w/v) paraformaldehyde for 10 minutes at room temperature or fixed with pre-chilled acetone for 5 minutes at 4 ˚C, and then permeabilized for 10 minutes with 0.2% Triton X-100 in PBS. Blocking was performed with 1% BSA in PBS for 1 hour, then incubated with indicated primary antibodies in PBS containing 1% BSA for 12 hours at 4˚C. After extensive rinses, cells were subsequently washed and incubated for 1 hour with secondary antibody at room temperature. Confocal images were acquired using a 100× oil objective with NA 1.40 on a Nikon confocal microscope (ECLIPSE Ti-C2, Japan). Images were obtained using the NIS-Elements AR 3.2 software provided by Nikon.

Inhibitor treatment

For inhibitor treatment, cells were loaded for 30 minutes with 2.5 μM rhod-2/am concomitant with indicated compounds, including 10 μM CCCP (Sigma), 10 μM oligomycin (Selleck), 2 μM rotenone (Sigma), 10 μM, 20 μM, and 30 μM 3′,4′-Dichlorobenzamil hydrochloride (DBZ; Sigma), respectively. Cells were then rinsed with medium containing DMSO or indicated compounds. The subsequent mitochondrial, melanosomal Ca^{2+} measurements were described above.

Journal of Cell Science • Accepted manuscript

Fluorescent Ca^{2+} imaging

Mouse melanocytes were seeded at 0.5×10^4 per well in Nunc™ Lab-Tek™ chambered cover glass (Thermo). For GFP-based Ca^{2+} indicator, the melanocytes were transfected with GCaMP6-TYR for 24 hours then were measured the fluorescence intensity by confocal microscope. For chemical-compound Ca^{2+} dyes, cells were loaded for 30 minutes with 2.5 μM rhod-2/am or X-rhod-1/am (Invitrogen), respectively. Following dye loading, cells were then rinsed with full-serum RIPM-1640 medium. For mitochondrial Ca^{2+} measurement, the cells were further incubated at 37°C for 20 minutes, then mounted in the cell chamber of the confocal microscope. For measurements of melanosomal Ca^{2+}, the cells were incubated at 37°C for 40 or 60 minutes, then mounted in the cell chamber.

Potassium depletion

Potassium depletion experiments were modified from previous protocols (Kiyoshima et al., 2011; Puri et al., 2001). In control group, melan-a melanocytes were maintained in 100% K^+-containing buffer (103.4 mM NaCl, 5.3 mM KCl, 23.8 mM $NaHCO_3$, 5.6 mM Na_2HPO_4, 0.4 mM $MgSO_4$, 0.423 mM $Ca(NO_3)2$, 11.1 mM D-glucose, pH 7.4, 2% BSA) and incubated with rhod-2/am. In 50%, 10% and 0% K^+-containing buffers, KCl was substituted by NaCl. In K^+-reduced or free groups, K^+ was gradually decreased to the indicated concentrations by following the order of 100%, 50%, 10%, and 0%. Taking the K^+-free group for example, melan-a melanocytes were incubated sequentially with 100%, 50%, 10%, K^+-containing buffers in 2 minute intervals and then incubated with rhod-2/AM in 0% K^+-containing buffer.

Journal of Cell Science • Accepted manuscript

Melanin measurement

Melanocytes were pretreated with tyrosinase inhibitor Phenylthiourea (PTU) (200 nM) for 3 days for depigmentation. Cells were further treated with PTU (positive control) and DMSO (negative control) or cultured in the presence of indicated compounds, 2 μM CCCP (Sigma), 5 μM oligomycin (Selleck), 0.4 μM rotenone (Sigma), 30 μM 3′,4′-Dichlorobenzamil hydrochloride (DBZ; Sigma), 10 μM CGP-37157 (Tocris), 100 mM leupeptin (Sigma) for 3 days. Melanin quantifications were performed as previously described (Wasmeier et al., 2006). The cells were harvested and washed in PBS, then pelleted and solubilized in 50 mM Tris-HCl, pH 7.4, 2 mM EDTA, 150 mM NaCl, 1 mM dithiothreitol, and protease inhibitors. Protein content of the supernatant was determined as optical density at 595 nm. Pigment was pelleted at 16,000 g for 10 minutes at 4°C, rinsed once in ethanol/ether (1:1), and dissolved in 2 M NaOH/20% dimethylsulfoxide at 60°C. Melanin content was measured as optical density at 492 nm and normalized to their protein content.

Statistical analysis

All data are shown as mean ± SEM in column bar graph, and as mean ± SD in scatter plot. Statistical analyses were performed with Student's t test or ANOVA with a post-Tukey's multiple comparison test. Differences were considered statistically significant when $P < 0.05$. Pearson's coefficients were calculated with the NIS-Elements AR 3.2 software (Nikon).

Journal of Cell Science • Accepted manuscript

Acknowledgements

We thank Drs. Richard Swank and Quan Chen for their comments and proofreading this manuscript.

Competing interests

The authors declare no competing interests for this work.

Author contributions

W. L., Z. Z. and A. W. designed the research and analyzed data. Z. Z. and J. G. performed research. E. V. S. guided melan-a culture. W. L. and Z. Z. wrote the paper.

Funding

This work was partially supported by grants from the National Natural Science Foundation of China (#31830054 (to W. L.); #81472871 (to A. W.); #91539204 (to W. L.)), the Ministry of Science and Technology of China (#2016YFC1000306) (to W. L.), and the Wellcome Trust (#108429) (to E. V. S.).

Journal of Cell Science • Accepted manuscript

REFERENCES

Altimimi, H. F., Szerencsei, R. T., and Schnetkamp, P. P. (2013). Functional and structural properties of the NCKX2 Na(+)-Ca (2+)/K (+) exchanger: a comparison with the NCX1 Na (+)/Ca (2+) exchanger. *Adv Exp Med Biol* **961**, 81-94.

Ammann, S., Schulz, A., Krageloh-Mann, I., Dieckmann, N. M., Niethammer, K., Fuchs, S., Eckl, K. M., Plank, R., Werner, R., Altmuller, J., et al. (2016). Mutations in AP3D1 associated with immunodeficiency and seizures define a new type of Hermansky-Pudlak syndrome. *Blood* **127**, 997-1006.

Babcock, D. F., Herrington, J., Goodwin, P. C., Park, Y. B., and Hille, B. (1997). Mitochondrial participation in the intracellular Ca^{2+} network. *J Cell Biol* **136**, 833-844.

Bennett, D. C., Cooper, P. J., and Hart, I. R. (1987). A line of non-tumorigenic mouse melanocytes, syngeneic with the B16 melanoma and requiring a tumour promoter for growth. *Int J Cancer* **39**, 414-418.

Berridge, M. J., Lipp, P., and Bootman, M. D. (2000). The versatility and universality of calcium signalling. *Nat Rev Mol Cell Biol* **1**, 11-21.

Berson, J. F., Harper, D. C., Tenza, D., Raposo, G., and Marks, M. S. (2001). Pmel17 initiates premelanosome morphogenesis within multivesicular bodies. *Mol Biol Cell* **12**, 3451-3464.

Berson, J. F., Theos, A. C., Harper, D. C., Tenza, D., Raposo, G., and Marks, M. S. (2003). Proprotein convertase cleavage liberates a fibrillogenic fragment of a resident glycoprotein to initiate melanosome biogenesis. *J Cell Biol* **161**, 521-533.

Blaustein, M. P., and Lederer, W. J. (1999). Sodium calcium exchange: Its physiological implications. *Physiol Rev* **79**, 763-854.

Burgoyne, T., Patel, S., and Eden, E. R. (2015). Calcium signaling at ER membrane contact sites. *Biochim Biophys Acta* **1853**, 2012-2017.

Bush, W. D., and Simon, J. D. (2007). Quantification of Ca(2+) binding to melanin supports the hypothesis that melanosomes serve a functional role in regulating calcium homeostasis. *Pigment Cell Res* **20**, 134-139.

Chi, A., Valencia, J. C., Hu, Z. Z., Watabe, H., Yamaguchi, H., Mangini, N. J., Huang, H., Canfield, V. A., Cheng, K. C., Yang, F., et al. (2006). Proteomic and bioinformatic characterization of the biogenesis and function of melanosomes. *J Proteome Res* **5**, 3135-3144.

Cox, D. A., Conforti, L., Sperelakis, N., and Matlib, M. A. (1993). Selectivity of inhibition of Na^{+}/Ca^{2+} exchange of heart-mitochondria by benzothiazepine cgp-37157. *J Cardiovasc Pharm* **21**, 595-599.

Daniele, T., Hurbain, I., Vago, R., Casari, G., Raposo, G., Tacchetti, C., and Schiaffino, M. V. (2014). Mitochondria and melanosomes establish physical contacts modulated by Mfn2 and involved in organelle biogenesis. *Curr Biol* **24**, 393-403.

Dell'Anna, M. L., Maresca, V., Briganti, S., Camera, E., Falchi, M., and Picardo, M. (2001). Mitochondrial impairment in peripheral blood mononuclear cells during the active phase of vitiligo. *J Invest Dermatol* **117**, 908-913.

Journal of Cell Science • Accepted manuscript

Ding, W. X., Ni, H. M., Li, M., Liao, Y., Chen, X., Stolz, D. B., Dorn, G. W., 2nd, and Yin, X. M. (2010). Nix is critical to two distinct phases of mitophagy, reactive oxygen species-mediated autophagy induction and Parkin-ubiquitin-p62-mediated mitochondrial priming. *J Biol Chem* **285**, 27879-27890.

Ezzedine, K., Eleftheriadou, V., Whitton, M., and van Geel, N. (2015). Vitiligo. *The Lancet* **386**, 74-84.

Fonteriz, R. I., de la Fuente, S., Moreno, A., Lobaton, C. D., Montero, M., and Alvarez, J. (2010). Monitoring mitochondrial [Ca(2+)] dynamics with rhod-2, ratiometric pericam and aequorin. *Cell Calcium* **48**, 61-69.

Garrity, A. G., Wang, W., Collier, C. M., Levey, S. A., Gao, Q., and Xu, H. (2016). The endoplasmic reticulum, not the pH gradient, drives calcium refilling of lysosomes. *eLife* **5**, 15887.

Ginger, R. S., Askew, S. E., Ogborne, R. M., Wilson, S., Ferdinando, D., Dadd, T., Smith, A. M., Kazi, S., Szerencsei, R. T., Winkfein, R. J., et al. (2008). SLC24A5 encodes a trans-Golgi network protein with potassium-dependent sodium-calcium exchange activity that regulates human epidermal melanogenesis. *J Biol Chem* **283**, 5486-5495.

Harman, D. (1972). The biologic clock: the mitochondria? *J Am Geriatr Soc* **20**, 145-147.

Hoashi, T., Muller, J., Vieira, W. D., Rouzaud, F., Kikuchi, K., Tamaki, K., and Hearing, V. J. (2006). The repeat domain of the melanosomal matrix protein PMEL17/GP100 is required for the formation of organellar fibers. *J Biol Chem* **281**, 21198-21208.

Hoashi, T., Watabe, H., Muller, J., Yamaguchi, Y., Vieira, W. D., and Hearing, V. J. (2005). MART-1 is required for the function of the melanosomal matrix protein PMEL17/GP100 and the maturation of melanosomes. *J Biol Chem* **280**, 14006-14016.

Hoogdijn, M. J., Smit, N. P., van der Laarse, A., van Nieuwpoort, A. F., Wood, J. M., and and Thody, A. J. (2003). Melanin has a Role in Ca2+Homeostasis in Human Melanocytes. *Pigment Cell Res* **16**, 127–132.

Ito, S., and Wakamatsu, K. (2011). Human hair melanins: what we have learned and have not learned from mouse coat color pigmentation. *Pigment Cell Melanoma Res* **24**, 63-74.

Kiyoshima, D., Kawakami, K., Hayakawa, K., Tatsumi, H., and Sokabe, M. (2011). Force- and Ca^{2+}-dependent internalization of integrins in cultured endothelial cells. *J Cell Sci* **124**, 3859-3870.

Kostic, M., Ludtmann, M. H., Bading, H., Hershfinkel, M., Steer, E., Chu, C. T., Abramov, A. Y., and Sekler, I. (2015). PKA Phosphorylation of NCLX Reverses Mitochondrial Calcium Overload and Depolarization, Promoting Survival of PINK1-Deficient Dopaminergic Neurons. *Cell Rep* **13**, 376-386.

Kushimoto, T., Basrur, V., Valencia, J., Matsunaga, J., Vieira, W. D., Ferrans, V. J., Muller, J., Appella, E., and Hearing, V. J. (2001). A model for melanosome biogenesis based on the purification and analysis of early melanosomes. *Proc Natl Acad Sci U S A* **98**, 10698-10703.

Laddha, N. C., Dwivedi, M., Mansuri, M. S., Gani, A. R., Ansarullah, M., Ramachandran, A. V., Dalai, S., and Begum, R. (2013). Vitiligo: interplay between oxidative stress and immune system. *Exp Dermatol* **22**, 245-250.

Lamason, R. L., Mohideen, M. A., Mest, J. R., Wong, A. C., Norton, H. L., Aros, M. C., Jurynec, M. J., Mao, X., Humphreville, V. R., Humbert, J. E., et al. (2005).

Journal of Cell Science • Accepted manuscript

SLC24A5, a putative cation exchanger, affects pigmentation in zebrafish and humans. *Science* **310**, 1782-1786.

Li, W., He, M., Zhou, H., Bourne, J. W., and Liang, P. (2006). Mutational data integration in gene-oriented files of the Hermansky-Pudlak Syndrome database. *Hum Mutat* **27**, 402-407.

Luongo, T. S., Lambert, J. P., Gross, P., Nwokedi, M., Lombardi, A. A., Shanmughapriya, S., Carpenter, A. C., Kolmetzky, D., Gao, E., van Berlo, J. H., et al. (2017). The mitochondrial Na^+/Ca^{2+} exchanger is essential for Ca^{2+} homeostasis and viability. *Nature* **545**, 93-97.

Minta, A., Kao, J. P., and Tsien, R. Y. (1989). Fluorescent indicators for cytosolic calcium based on rhodamine and fluorescein chromophores. *J Biol Chem* **264**, 8171-8178.

Morice-Picard, F., Lasseaux, E., Francois, S., Simon, D., Rooryck, C., Bieth, E., Colin, E., Bonneau, D., Journel, H., Walraedt, S., et al. (2014). SLC24A5 mutations are associated with non-syndromic oculocutaneous albinism. *J Invest Dermatol* **134**, 568-571.

Niel, G. V., Charrin, S., Simoes, S., Romao, M., Rochin, L., Saftig, P., Marks, M. S., Rubinstein, E., and Raposo, G. (2011). The tetraspanin CD63 regulates ESCRT-independent and -dependent endosomal sorting during melanogenesis. *Dev Cell* **21**, 708-721.

Palty, R., Silverman, W. F., Hershfinkel, M., Caporale, T., Sensi, S. L., Parnis, J., Nolte, C., Fishman, D., Shoshan-Barmatz, V., Herrmann, S., et al. (2010). NCLX is an essential component of mitochondrial Na+/Ca2+ exchange. *Proc Natl Acad Sci U S A* **107**, 436-441.

Patel, S., and Docampo, R. (2010). Acidic calcium stores open for business: expanding the potential for intracellular Ca2+ signaling. *Trends Cell Biol* **20**, 277-286.

Puri, V., Watanabe, R., Singh, R. D., Dominguez, M., Brown, J. C., Wheatley, C. L., Marks, D. L., and Pagano, R. E. (2001). Clathrin-dependent and -independent internalization of plasma membrane sphingolipids initiates two Golgi targeting pathways. *J Cell Biol* **154**, 535-547.

Raposo, G., Tenza, D., Murphy, D. M., Berson, J. F., and Marks, M. S. (2001). Distinct protein sorting and localization to premelanosomes, melanosomes, and lysosomes in pigmented melanocytic cells. *J Cell Biol* **152**, 809-823.

Rizzuto, R., Marchi, S., Bonora, M., Aguiari, P., Bononi, A., De Stefani, D., Giorgi, C., Leo, S., Rimessi, A., Siviero, R., et al. (2009). Ca(2+) transfer from the ER to mitochondria: when, how and why. *Biochim Biophys Acta* **1787**, 1342-1351.

Rizzuto, R., Pinton, P., Carrington, W., Fay, F. S., Fogarty, K. E., Lifshitz, L. M., Tuft, R. A., and Pozzan, T. (1998). Close contacts with the endoplasmic reticulum as determinants of mitochondrial Ca2+ responses. *Science* **280**, 1763-1766.

Rogasevskaia, T. P., Szerencsei, R. T., Jalloul, A. H., Visser, F., Winkfein, R. J., and Schnetkamp, P. P. M. (2019). Cellular localization of the K(+) -dependent Na(+) -Ca(2+) exchanger NCKX5 and the role of the cytoplasmic loop in its distribution in pigmented cells. *Pigment Cell Melanoma Res* **32**, 55-67.

Schnetkamp, P. P. (2013). The SLC24 gene family of Na^+/Ca^{2+}-K^+ exchangers: from sight and smell to memory consolidation and skin pigmentation. *Mol Aspects Med* **34**, 455-464.

Journal of Cell Science • Accepted manuscript

Seiberg, M. (2013). Age-induced hair greying - the multiple effects of oxidative stress. *Int J Cosm Sci* **35**, 532-538.

Shumilina, E., Xuan, N. T., Matzner, N., Bhandaru, M., Zemtsova, I. M., and Lang, F. (2010). Regulation of calcium signaling in dendritic cells by 1,25-dihydroxyvitamin D3. *FASEB J* **24**, 1989-1996.

Sitaram, A., and Marks, M. S. (2012). Mechanisms of protein delivery to melanosomes in pigment cells. *Physiology (Bethesda)* **27**, 85-99.

Thomas, G. (2002). Furin at the cutting edge: From protein traffic to embryogenesis and disease. *Nat Rev Mol Cell Bio* **3**, 753-766.

Vance, J. E. (1990). Phospholipid synthesis in a membrane fraction associated with mitochondria. *J Biol Chem* **265**, 7248-7256.

Wasmeier, C., Romao, M., Plowright, L., Bennett, D. C., Raposo, G., and Seabra, M. C. (2006). Rab38 and Rab32 control post-Golgi trafficking of melanogenic enzymes. *The J Cell Biol* **175**, 271-281.

Wei, A. H., and Li, W. (2013). Hermansky-Pudlak syndrome: pigmentary and non-pigmentary defects and their pathogenesis. *Pigment Cell Melanoma Res* **26**, 176-192.

Wei, A. H., Zang, D. J., Zhang, Z., Liu, X. Z., He, X., Yang, L., Wang, Y., Zhou, Z. Y., Zhang, M. R., Dai, L. L., et al. (2013). Exome sequencing identifies SLC24A5 as a candidate gene for nonsyndromic oculocutaneous albinism. *J Invest Dermatol* **133**, 1834-1840.

Yasumoto, K., Watabe, H., Valencia, J. C., Kushimoto, T., Kobayashi, T., Appella, E., and Hearing, V. J. (2004). Epitope mapping of the melanosomal matrix protein gp100 (PMEL17): rapid processing in the endoplasmic reticulum and glycosylation in the early Golgi compartment. *J Biol Chem* **279**, 28330-28338.

Journal of Cell Science • Accepted manuscript

Figures

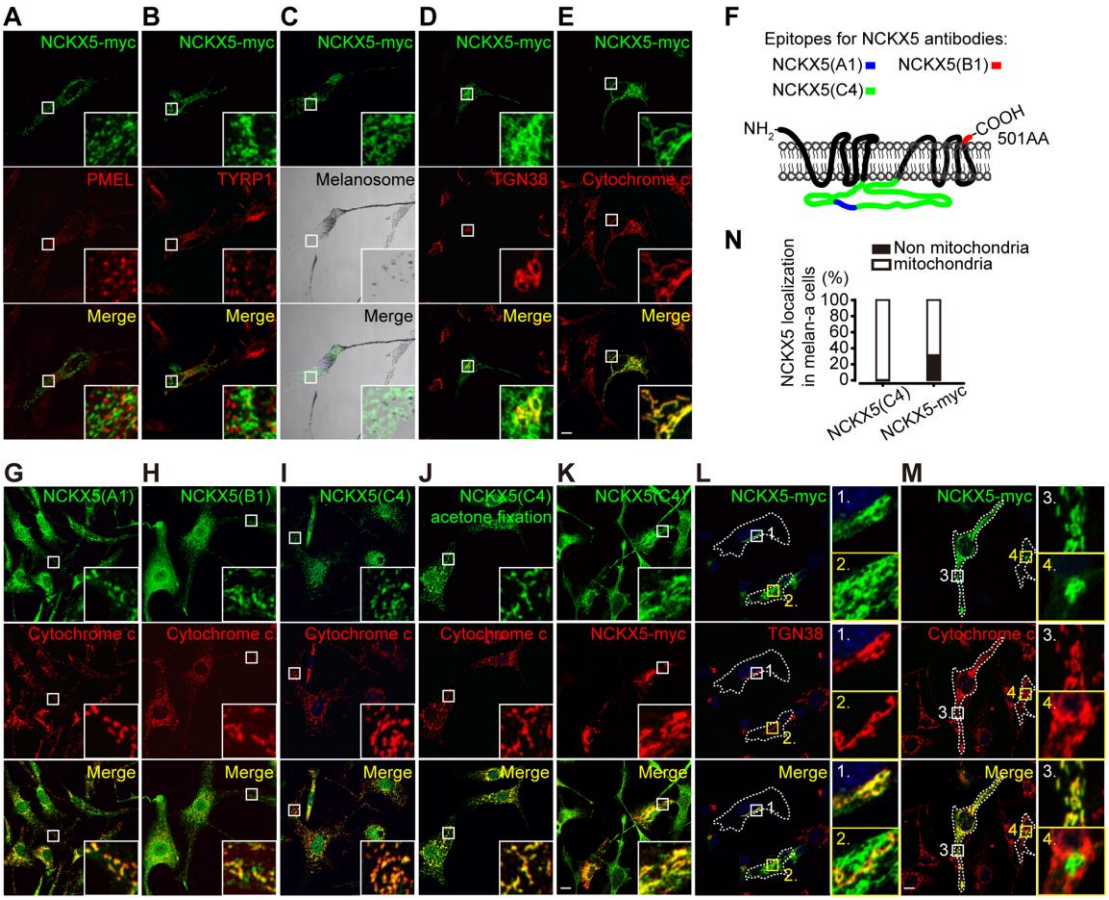

Fig. 1. NCKX5 is predominantly localized to mitochondria.

(**a-e”**) Melan-a melanocytes were transfected with the NCKX5-myc transgene and incubated with antibodies to PMEL (**a-a”**), TYRP1 (**b-b”**), TGN38 (**d-d”**), cytochrome c (**e-e”**). The bright field of pigmented melanosomes was visualized (**d-d”**). Insets show 5× magnified images of the boxed region. Scale bar, 10 μm. (**f**) Schematic of the pepdides were choosed to generate NCKX5 polyclonal anti-sera. (**g-k”**) Melan-a melanocytes were co-labeled with NCKX5 polyclonal anti-sera and cytochrome c: NCKX5(A1) (g-g’’); NCKX5(B1) (h-h’’); NCKX5(C4) (i-i’’); NCKX5(C4) acetone fixation (j-j’’). Insets show 5× magnified images of the boxed region. Scale bar, 10 μm.

Journal of Cell Science • Accepted manuscript

(**k-k”**) Melan-a melanocytes were transfected with the NCKX5-myc transgene and co-labeled with NCKX5 polyclonal anti-sera. (**l-m”**) Melan-a melanocytes were transfected with the NCKX5-myc transgene and incubated with antibodies to TGN (l-l’’) and cytochrome c (m-m’’). Outlines of cells are indicated by white lines. Insets show 6× magnified images of the boxed region. Scale bar, 10 μm. (**n**) The percentage of the NCKX5 (anti-NCKX5-C4 and NCKX5-myc) co-localized with anti-cytochrome c. n=265 and 88 melanocytes, respectively.

Journal of Cell Science • Accepted manuscript

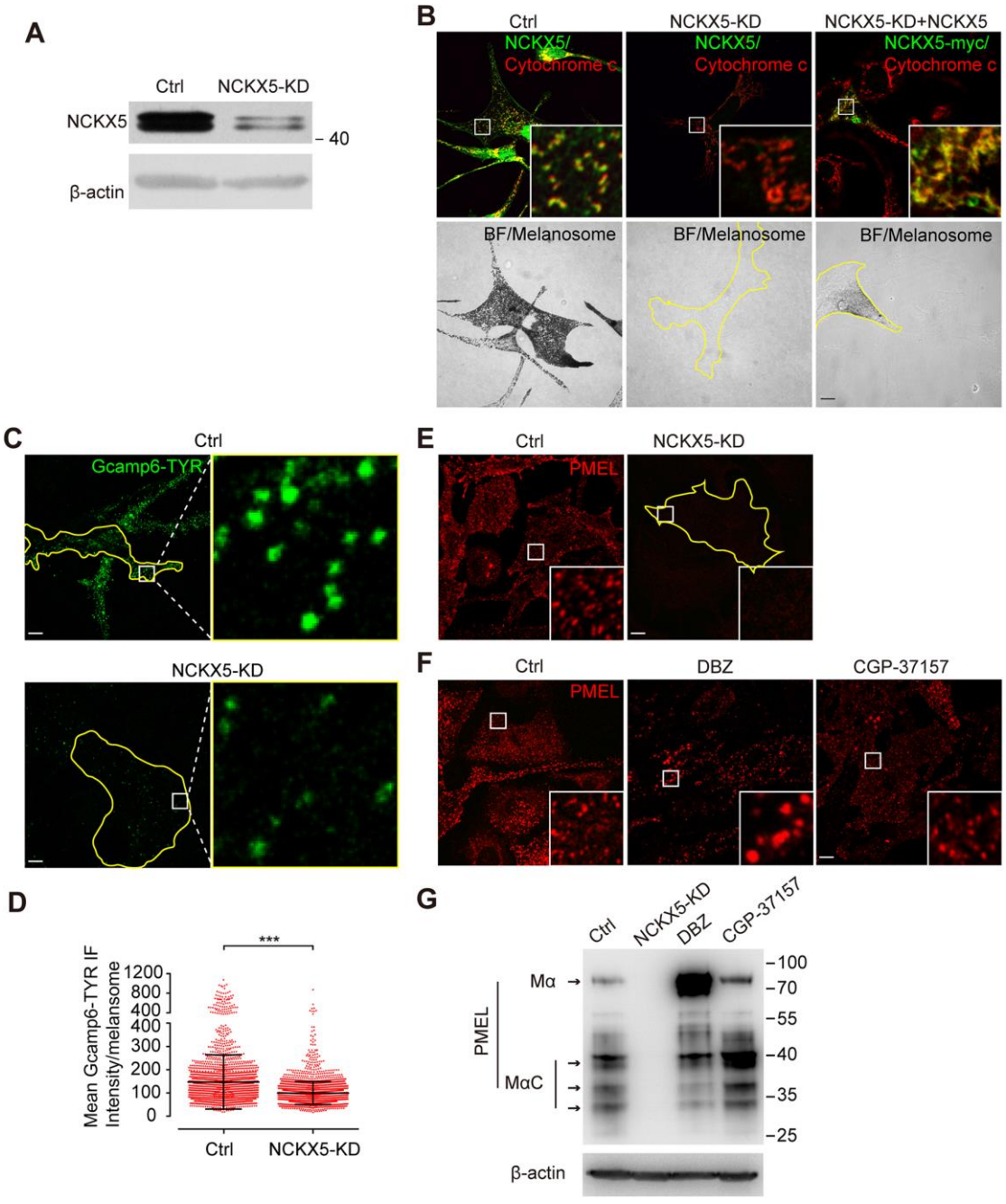

Fig. 2. Loss of NCKX5 compromises melanosomal Ca^{2+} concentration, melanosomal protein PMEL expression and melanin production.

(**a**) Western blot analysis of lysates from melan-a melanocytes stably expressed control shRNA (Ctrl) and melan-a melanocytes stably expressed *Nckx5* shRNA (NCKX5-KD) using NCKX5 polyclonal anti-sera. β-actin antibody is a loading control. (**b-g**) Confocal

Journal of Cell Science • Accepted manuscript

immunofluorescent images of Ctrl melanocytes, NCKX5-KD melanocytes and NCKX5-KD melanocytes transfected with NCKX5-myc by co-labeling with NCKX5 polyclonal anti-sera and cytochrome c antibody. The bright field (BF) of pigmented melanosomes was visualized. Outlines of cells are indicated by yellow lines. Insets show 6× magnified images of the boxed region. Scale bar, 10 μm. (**h-k**) Confocal immunofluorescent images of melan-a wild-type melanocytes (WT) and NCKX5-KD melanocytes transfected with GCaMP6-TYR. Outlines of cells are indicated by yellow lines. Insets show 12× magnified images of the boxed region, Scale bar, 10 μm. (**l**) Quantification of mean fluorescent intensity of GCaMP6-TYR in WT and NCKX5-KD group, n = 2,336, and 2,723 melanosomes, respectively. Each point represents the mean fluorescent intensity of GCaMP6-TYR labelled single melanosome. ***$P < 0.001$. (**m, n**) Confocal immunofluorescent images of melanocytes labeled with melanosomal protein PMEL in Ctrl and NCKX5-KD melanocytes. Insets show 6× magnified images of the boxed region. Scale bar, 10 μm. (**o-q**) Confocal immunofluorescent images of melanocytes incubated with corresponding compounds, DMSO, DBZ (30μM), CGP-37157 (10 μM) by labeling with melanosomal protein PMEL. Outlines of cells are indicated by yellow lines. Insets show 6× magnified images of the boxed region. Scale bar, 10 μm. (**r**) Western blot analysis of lysates of Ctrl melanocytes, NCKX5-KD melanocytes, melan-a melanocytes incubated with DBZ (30μM) or CGP-37157 (10 μM) using PMEL antibody. β-actin antibody as a loading control.

Journal of Cell Science • Accepted manuscript

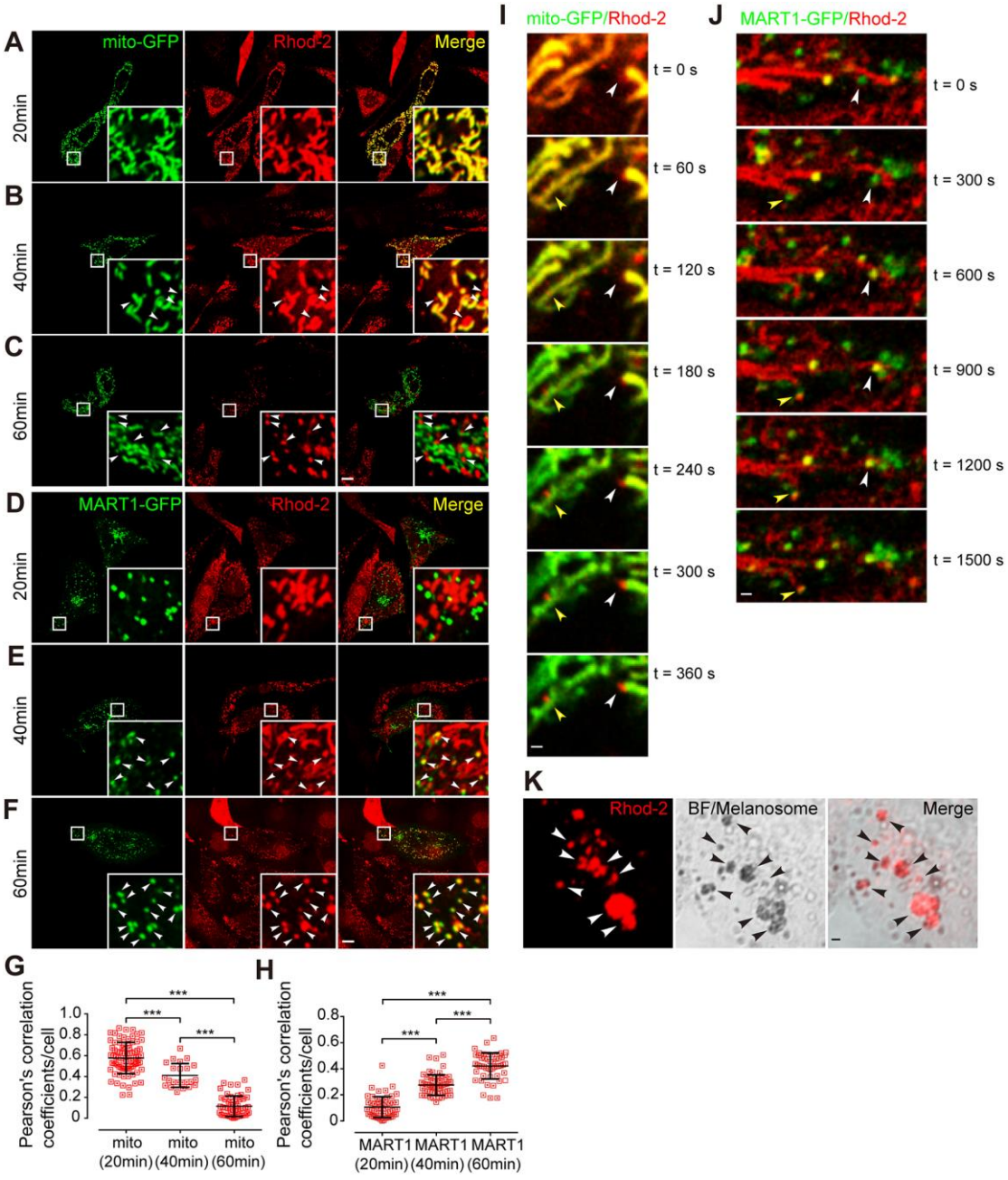

Fig. 3. Rhod-2 signals efflux from mitochondria and influx into melanosomes.

(**a-c”**) Colocalization of mito-GFP with Ca^{2+} indicator rhod-2 signals at indicated time points after dye loading and washing with medium (20 min, a-a’’; 40 min, b-b’’; 60 min, c-c’’) was analyzed by live-cell imaging in melan-a cells. Arrowheads, rhod-2 fluorescent dots separated from mito-GFP. Insets show 6× magnified images of the boxed region.

Journal of Cell Science • Accepted manuscript

Scale bar, 10 μm. (**d**) Colocalization analysis in (a'', b'', c''), n = 79, 23, and 54 cells, respectively. ***$P < 0.001$. (**e-g''**) Colocalization of MART1-GFP with Ca^{2+} indicator rhod-2 signals at indicated time points after dye loading and washing with medium (20 min, e-e''; 40 min, f-f''; 60 min, g-g'') in melan-a cells. Arrowheads, rhod-2 fluorescent dots colocalized with MART1-GFP. Insets show 6× magnified images of the boxed region. Scale bar, 10 μm. (**h**) Colocalization analysis in (e'', f'', g''), n = 57, 58, and 50 cells, respectively. ***$P < 0.001$. (**i**) Time course of rhod-2 separation from mito-GFP. Arrowheads, rhod-2 fluorescent dots separated from mito-GFP. Scale bar, 1 μm. (**j**) Time course of rhod-2 colocalization with MART1-GFP. Arrowheads, rhod-2 fluorescent dots colocalized with MART1-GFP. Scale bar, 1 μm. (**k-m**) Rhod-2 fluorescent dots colocalized with melanosomal granules. Melan-a melanocytes were labeled with rhod-2 and visualized by BF for pigmented melanosomes. Arrowheads, rhod-2 fluorescent dots colocalized with melanosomes. Scale bar, 1 μm.

Journal of Cell Science • Accepted manuscript

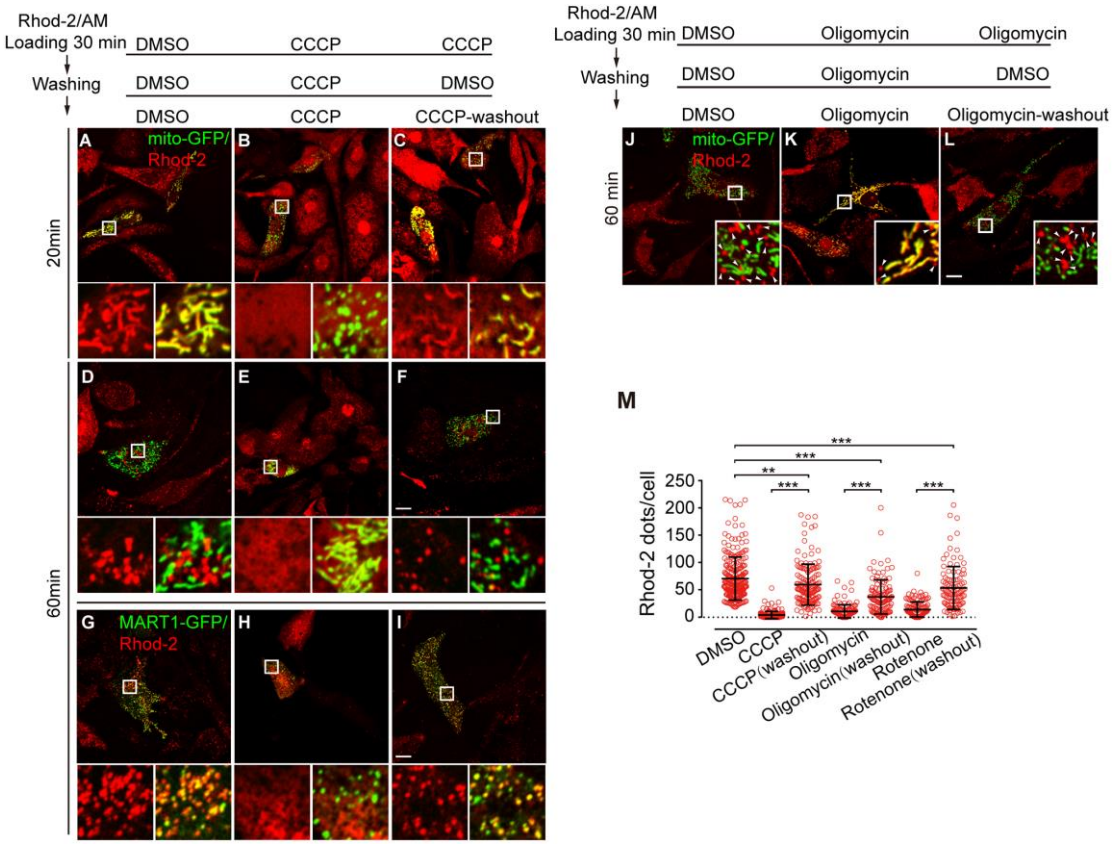

Fig. 4. Functional mitochondria are required for mitochondrial rhod-2 transfer to melanosomes.

(**a-f**) Confocal immunofluorescent images of melan-a melanocytes transfected with mito-GFP and labeled with rhod-2 in the presence of DMSO (control) or 10 μM CCCP respectively, all the indicated time points were time after dye loading and washed with indicated medium. Insets show 6× magnified images of the boxed region. Scale bar, 10 μm. (**g-i**) Confocal immunofluorescent images of melan-a melanocytes transfected with MART1-GFP and labeled with rhod-2 in the presence of DMSO (control) or 10 μM CCCP respectively, 60 min after dye loading and washed with indicated medium. Insets show 6× magnified images of the boxed region. Scale bar, 10 μm. (**j**) Quantification of rhod-2 dots (60 min after wash) in each treatment, n = 245, 170, 149, 123, 117, 130, and

Journal of Cell Science • Accepted manuscript

107 cells, respectively. Each point represents the number of rhod-2 dots in a single cell. **$P < 0.01$; ***$P < 0.001$. (**k-m**) Confocal immunofluorescent images of melanocytes transfected with mito-GFP then labeled with rhod-2 in the presence of indicated compounds (60 min after dye loading and washing with indicated medium): DMSO (a); oligomycin 10 μM (b); oligomycin 10 μM washout (c). Arrowheads, rhod-2 dots separated from mito-GFP. Insets show 6× magnified images of the boxed region. Scale bar, 10 μm.

Journal of Cell Science • Accepted manuscript

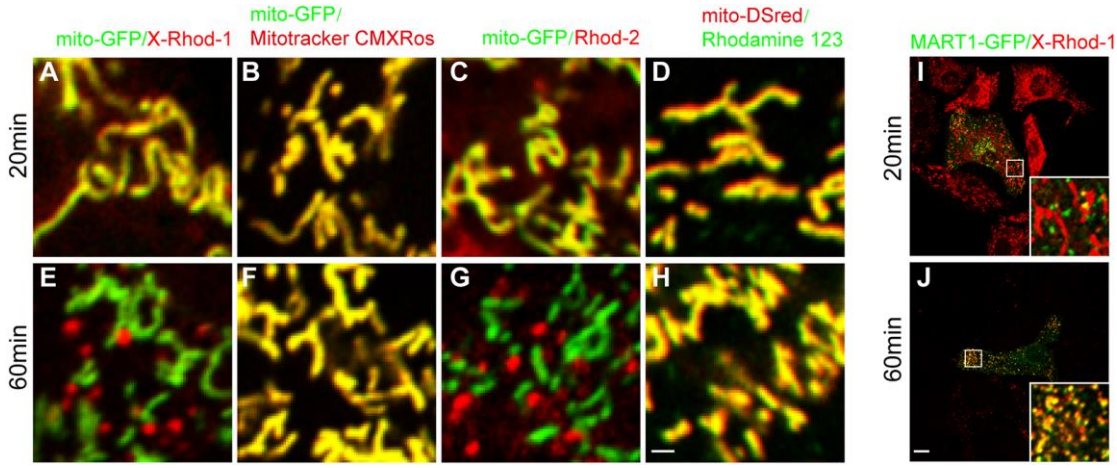

Fig. 5. X-rhod-1 and rhod-2 specifically efflux from mitochondria and influx into melanosomes.

(**a-d**) Images of melanocytes transfected with mito-GFP and labeled with indicated chemical-compound dyes (20 min after dye loading and washing with medium): X-rhod-1(a); mitotracker CMXRos (b); rhod-2 (c); rhodamine 123 (d). Scale bar, 10 μm. (**e-h**) Images of melanocytes transfected with mito-GFP and labeled with indicated chemical-compound dyes (60 min after dye loading and washing with medium): X-rhod-1(a); mitotracker CMXRos (b); rhod-2 (c); rhodamine 123 (d). Scale bar, 10 μm. (**j**) Images of melanocytes transfected with MART1-GFP and labeled with X-rhod-1 at 20 min after dye loading and washing with medium. Scale bar, 10 μm. (**k**) Images of melanocytes transfected with MART1-GFP and labeled with X-rhod-1 at 60min after dye loading and washing with medium. Scale bar, 10 μm.

Journal of Cell Science • Accepted manuscript

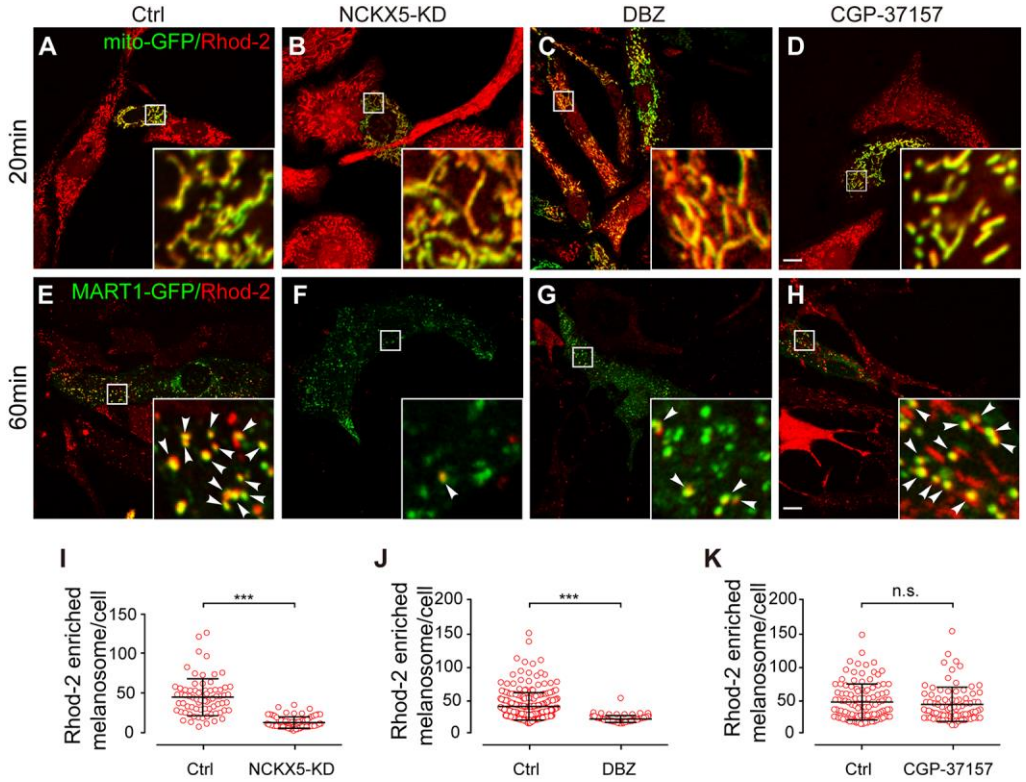

Fig. 6. NCKX5 and NCKX activity are required for rhod-2 signal accumulation in melanosomes.

(**a-d**) Images of corresponding melanocytes transfected with mito-GFP and labeled with rhod-2 (20 min after dye loading and washing with medium): control (a); NCKX5-KD (b); DBZ (30μM) (c); CGP-37157 (10 μM) (d). Insets show 6× magnified images of the boxed region. Scale bar, 10 μm. (**e-h**) Images of corresponding melanocytes transfected with MART1-GFP and labeled with rhod-2 (60 min after dye loading and washing with medium): control (e); NCKX5-KD (f); DBZ (30μM) (g); CGP-37157 (10 μM) (h). Insets show 6× magnified images of the boxed region. Scale bar, 10 μm. (**i)** Quantification of rhod-2 fluorescent dots colocalized with MART1-GFP (60 min after washing) in control and NCKX5-KD group. n = 74, and 78 cells, respectively. Each point represents the number of rhod-2 and MART1-GFP co-labeled dots in a single cell. ***$P < 0.001$. (**j**)

Journal of Cell Science • Accepted manuscript

Quantification of rhod-2 fluorescent dots colocalized with MART1-GFP (60 min after washing) in control and DBZ (30μM) group. n = 268, and 94 cells, respectively. Each point represents the number of rhod-2 and MART1-GFP co-labeled dots in a single cell. ***$P < 0.001$. (**k**) Quantification of rhod-2 fluorescent dots colocalized with MART1-GFP (60 min after washing) in control and CGP-37157 (10 μM) group, n = 114, and 86 cells, respectively. Each point represents the number of rhod-2 and MART1-GFP co-labeled dots in a single cell. n.s., not significant.

Journal of Cell Science • Accepted manuscript

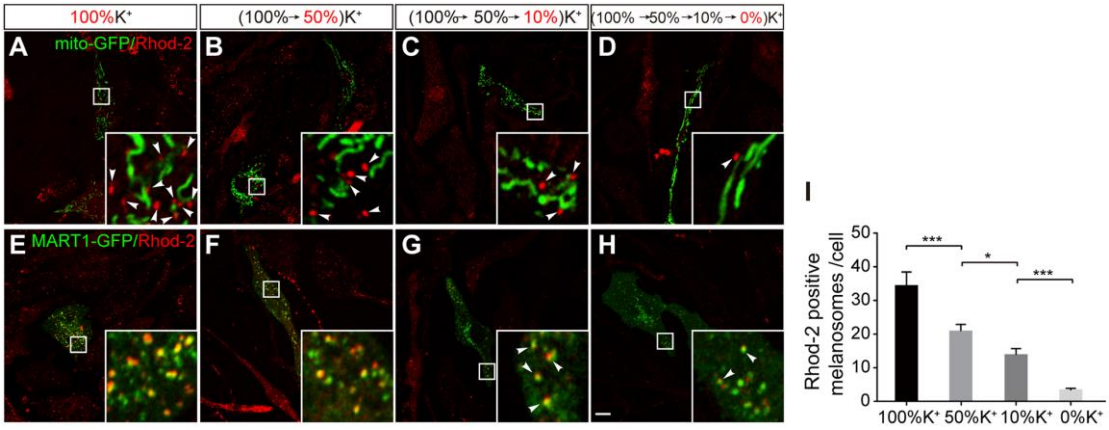

Fig. 7. NCKX activity is required for rhod-2 loading in melanosomes.

(**a-d**) Images of melan-a melanocytes transfected with mito-GFP and rinsed with 100% K^+-containing or K^+-declining buffers, then labeled with rhod-2 (60 min after wash), the final K^+ concentration in each treatment were presented in red: 100% K^+ (control, g); 50% K^+ (h); 10% K^+ (i); 0% K^+ (j). (**e-h**) Images of melan-a melanocytes transfected with MART1-GFP and rinsed with 100% K^+-containing or K^+-declining buffers, then labeled with rhod-2 (60 min after wash), the final K^+ concentration in each treatment were presented in red: 100% K^+ (control, g); 50% K^+ (h); 10% K^+ (i); 0% K^+ (j). **(i)** Quantification of rhod-2 colocalized with MART1-GFP in a single melanocyte in (e-h), n = 96, 111, 163, and 147 cells, respectively. *P < 0.05; ***P < 0.001.

Journal of Cell Science • Accepted manuscript

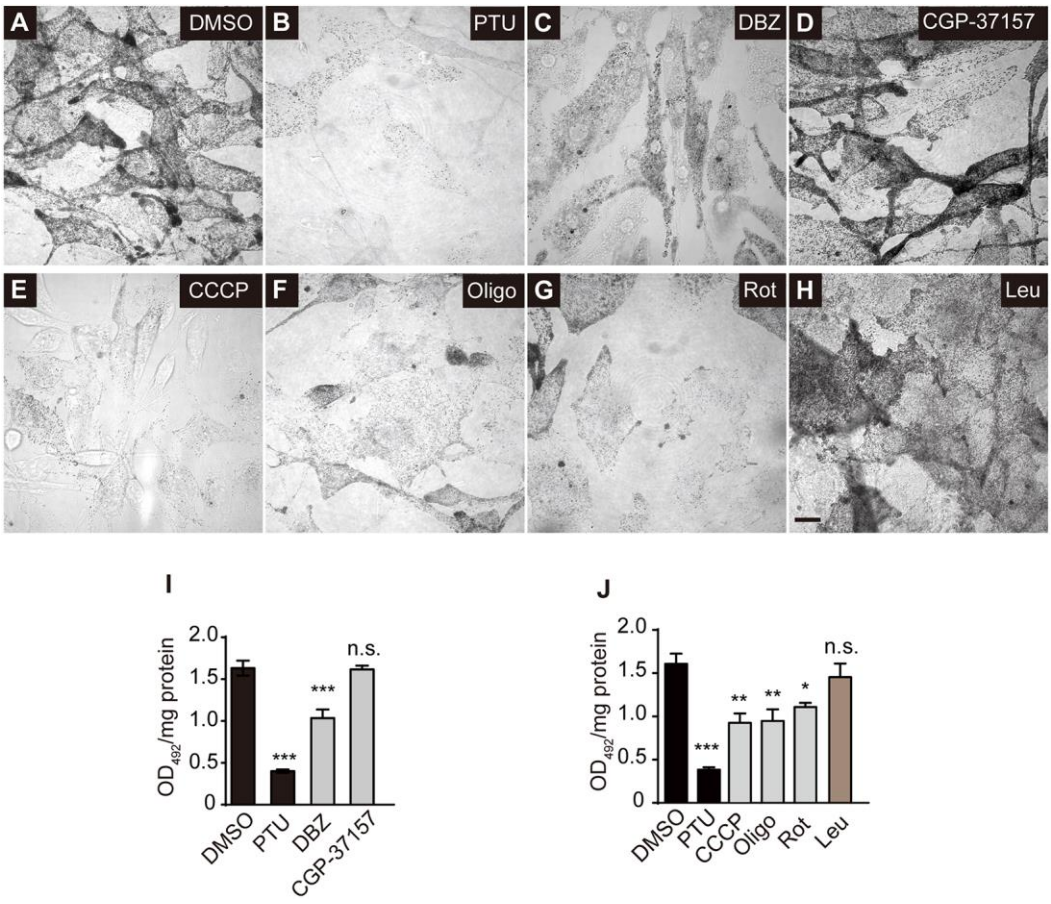

Fig. 8. NCKX activity and functional mitochondria are required for melanosomal pigment production.

(**a-h**) Confocal bright field images of melan-a melanocytes incubated with corresponding compounds for 72 hours: DMSO (a); phenylthiourea (PTU, 200 nM) (b); DBZ (30μM) (c); CGP-37157 (10 μM) (d); CCCP (2 μM) (e); Oligomycin (Oligo, 5 μM) (f); Rotenone (Rot, 0.4 μM) (g); Leupeptin (Leu, 100 mM) (h). Scale bar, 10 μm. (**i**) Melanin quantification assays for mlanocytes incubated with PTU (200 nM), DBZ (30μM); CGP-37157 (10μM). Melanin content was assayed by measuring optical density at 492 nm (OD_{492}). Assays were performed in triplicate. Data shown are means ± SEM of the number of triplicate experiments. n.s., not significant; ***$P < 0.001$. (**j**) Melanin quantification assays for melanocytes incubated with PTU (200 nM); CCCP (2 μM);

Journal of Cell Science • Accepted manuscript

Oligo (5 μM); Rot (0.4 μM); Leu (100 mM). Melanin content was assayed by measuring optical density at 492 nm (OD_{492}). Assays were performed in triplicate. Data shown are means ± SEM of the number of triplicate experiments. n.s., not significant; *$P < 0.05$; **$P < 0.01$; ***$P < 0.001$.

Journal of Cell Science • Accepted manuscript